Title
HYPERCRYOGENIC DETECTOR-FET UNIT -- CORE OF A HIGH-RESOLUTION SPECTROMETER

Authors
Elad, E.
Nakamura, M.

Publication Date
1968-02-07

University of California

Ernest O. Lawrence Radiation Laboratory

HYPERCRYOGENIC DETECTOR - FET UNIT--
CORE OF A HIGH-RESOLUTION SPECTROMETER

E. Elad and M. Nakamura

February 7, 1968

DISCLAIMER

For the 11th Scintillation and Semiconductor Counter Symposium, Washington, D. C., Feb. 28, 29, and March 1, 1968

UCRL-17901
Preprint

UNIVERSITY OF CALIFORNIA

Lawrence Radiation Laboratory
Berkeley, California

AEC Contract No. W-7405-eng-48

HYPERCRYOGENIC DETECTOR-FET UNIT--CORE OF A HIGH-RESOLUTION SPECTROMETER

E. Elad and M. Nakamura

February 7, 1968

HYPERCRYOGENIC DETECTOR–FET UNIT--CORE OF HIGH-RESOLUTION SPECTROMETER

E. ELAD AND M. NAKAMURA
Lawrence Radiation Laboratory
University of California
Berkeley, California

SUMMARY

A hypercryogenic high-resolution x-ray and γ-ray spectrometer is described. The spectrometer consists of a lithium-drifted germanium detector and a germanium-junction field-effect transistor (JFET) preamplifier. The detector is operated at its optimum temperature, which is in the range of 10-30° K. The JFET's are operated at liquid helium temperature. This results in 0.28 keV FWHM preamplifier resolution with a slope of 0.018 keV/pF. Resolutions of the order of 0.4 keV are obtained with low capacitance detectors for low-energy x rays. The γ rays of ^{57}Co are measured with 0.68 keV FWHM.

The described spectrometer was used to study some aspects of the trapping effects in germanium detectors.

INTRODUCTION

Semiconductor radiation detectors are the basis for high-resolution spectrometers. For several years the weak link in semiconductor spectrometers was the input stage of the preamplifier. The noise of that stage limited the signal-to-noise ratio of the system and hampered the excellent resolving capabilities of the detector. This situation changed with the technological advances in fabrication of junction field-effect transistors (JFET). Nowadays well-optimized silicon JFET's having high g_m/C_g ratios are increasingly available. Recently also a germanium planar JFET was manufactured, and work continues on high-mobility III - V compound FET's. Field-effect transistors have favorable cryogenic characteristics for low-noise amplification. It is therefore no surprise that with the availability of the new devices several high-resolution cryogenic preamplifiers using silicon JFET's were built.[1-3] A germanium FET preamplifier[4] was recently added to the list of high-resolution instruments.

The availability of high-resolution preamplifiers increased the importance of seeking optimum operating conditions for the germanium detectors. In the present spectrometers, germanium detectors are operated above 77° K, sometimes as high as 100° K--in particular, when supported by electrically insulated holders. This method of operation, namely cooling the detector with liquid nitrogen, is convenient but certainly not optimum. Information on the optimum operating temperature of the germanium detectors, mainly for high-energy γ rays was reported by E. Sakai et al.[5] They found the optimum temperature in the range of 20-40° K.

This paper describes a hypercryogenic high-resolution x-ray and γ-ray spectrometer. The spectrometer consists of a lithium-drifted germanium detector and a germanium junction field-effect transistor (JFET) preamplifier. Optimum operating temperature for the germanium detector was found for low-energy radiation. That temperature is in the range between 10 to 35° K and it depends on the particular detector and its history.

The JFET's are operated at liquid-helium temperature, to attain their high-gain, low-noise characteristics, superior to the well-optimized and selected silicon devices. Pulse generator resolution of the preamplifier for zero external capacitance is 0.28 keV FWHM (Ge), with a slope of 0.018 keV/pF.

Several detectors were used in the spectrometer. Low-capacitance, thin-window detectors give resolutions of the order of 0.4 keV for low-energy x rays (5-15 keV), 0.5 keV for higher energy x rays (50 keV), and 0.68 keV for medium-energy γ rays (122-keV ^{57}Co). A medium capacitance (12 pF), thick-window detector recorded the ^{57}Co lines with 0.93 keV FWHM.

GERMANIUM DETECTORS

Germanium detectors are used extensively in nuclear spectroscopy. Their principles of operation are fairly well understood and several review articles have been written covering the various aspects of detection with these counters.[6-8] In the following we shall concentrate on the temperature-dependent characteristics of the compensated germanium detectors.

The equivalent circuit of a lithium-drifted germanium detector is given in Fig. 1. The current generator I_ℓ represents the total leakage current of the device, C the junction capacitance, and R the resistance of the undepleted region. The leakage current of a p-n junction consists of diffusion and generation bulk components and a surface component. Radiation detectors require thick depletion layers which are realized by lithium compensation forming p-i-n structures. In these devices only the generation components in the bulk and the surface will be significant. The generation current in the bulk space charge layer is given by[9]

$$I_g = qAW \frac{n_i}{2\tau}, \qquad (1)$$

where q is the charge of an electron, A the area of the diode, W the thickness of the depletion layer, n_i the density of thermally generated carriers, and τ the lifetime of the carriers. It was assumed that the generating centers are in the middle of the energy gap and that the lifetimes of holes and electrons are equal. The lifetime τ is given by

$$\tau = \frac{1}{\sigma \cdot v_{th} \cdot N_g}, \qquad (2)$$

where σ is the capture cross section of the generation-recombination centers, v_{th} the thermal velocity, and N_g the concentration of generation-recombination centers. The main temperature dependence of I_g comes through n_i and the lifetime τ. For germanium,

$$n_i = 1.76 \cdot 10^{16}\ T^{3/2} \exp\left(-\frac{4550}{T}\right), \qquad (3)$$

decreasing strongly with temperature. Unfortunately, there is little information on carrier lifetimes (or capture cross sections) at cryogenic temperatures. There is evidence of increased trapping of carriers at liquid-helium temperatures. This will reduce the effective lifetime as the probability of detrapping at these temperatures is very small. Therefore, the increased trapping will cause deterioration of resolution but will not increase the generation current I_g. From this we can expect that the generation current will decrease with temperature below 77°K.

The surface component of the leakage current is calculated in a similar way to the one used for bulk generation [Eq. (1)], assuming a completely depleted surface. The surface generation component is given by[10]

$$I_s = \frac{1}{2} q n_i s_0 A_s, \qquad (4)$$

where A_s is the surface area and s_0 the surface recombination velocity expressed by

$$s_0 = \sigma_s \cdot v_{th} \cdot N_{gs}, \qquad (5)$$

with the parameters as in Eq. (2), but for the surface. The surface current has the same temperature dependence as I_g through n_i and s_0. The only difference is the indirect temperature dependence of N_{gs} in the case of nonencapsulated germanium detectors. Liquid-helium cooling acts in effect as a cryopump improving the vacuum of the cryostat considerably. Therefore, the probability of adsorption of polar molecules on the surface is reduced, causing a decrease in N_{gs}.

To summarize, theoretically, the leakage current I_ℓ should be decreased significantly by reducing the temperature of the detector from 77°K to 10-20°K. The exact measurement of I_ℓ is complicated because of the small amplitude of this current. It requires a carefully shielded measuring setup and a high-voltage connector with resistance to ground higher than $10^{16}\ \Omega$.

The capacitance of a germanium detector is only weakly temperature dependent. It is inversely proportional to the thickness of the intrinsic region, which will be temperature independent in the case of perfect compensation. Otherwise, when some ionized impurities are still present in the compensated region, the capacitance will be higher than expected. Decreasing the temperature into the liquid-helium range will cause deionization of these impurities, which may have shallow (boron) or deep (copper) energy levels. This will consequently decrease the capacitance. Also deionization of the impurities in the uncompensated p-region will increase the intrinsic layer and decrease the capacitance.

Measurements were made on fully (2 pF) and partially (10 pF) compensated detectors. The capacitance of these devices at 500 V decreased between 30 and 10°K by 1% and 3%, respectively.

The resistance R has two parasitic effects on the performance of a germanium detector. It exhibits thermal noise ($\sqrt{4kTR}$) and slows down the rise time of the output pulse. The resistance R will decrease with temperature between 77 and 10°K, as the mobility of lightly doped germanium increases in that temperature range.[4] Consequently, lowering the temperature of the detector reduces both parasitic effects of R.

Summarizing, we can say that the noise sources of the detector, both shot and thermal, are reduced and the signal-to-noise ratio improved, as its temperature is lowered below 77°K. Additional improvement in the performance of a germanium detector at the hypercryogenic temperatures is made possible by the reduced value of the leakage current. Higher bias voltage may now be applied, thus improving charge collection statistics and reducing the capacitance of the detector and, therefore, further improving its resolution.

In the above, the advantages of hypercryogenic operation were outlined, but not all the characteristics of the detector improve at reduced temperature. The main problem that arises is the increased trapping of carriers, thus causing poor collection statistics and deterioration of the resolution. Therefore, optimum temperature exists for the achievement of best resolution. This temperature depends heavily on the amount of trapping centers and their characteristics and, therefore, will be a function of the history of the detector and the energy of the ionizing radiation. Some aspects of the trapping and detrapping effects are described in a later section.

THE PREAMPLIFIER

The following preamplifier circuit with minor modifications was described elsewhere.[4] The input stage of this circuit and the coupling network to the germanium detector are shown in Fig. 2. The input stage consists of two p-channel germanium JFET's type TIXM12 in cascode. The transconductance of that FET as a function of temperature is given in Fig. 3. Maximum transconductance for low-current units is obtained at 4.2°K (transistor case temperature). Low-current FET's operated at liquid-helium temperatures are employed in the input stage. The FET's are actually in the liquid to minimize their 1/f noise, which increases strongly with temperature, and to insure stability of the gain. The FET's are connected to the passive elements of the stage through low-capacitance feedthroughs. They are operated with zero gate-to-source bias and V_{DS} of approximately 2 V. The low V_{DS} prevents a large component of avalanche-type noise, but also causes relatively large junction capacitances. The germanium JFET's have almost perfect noise uniformity at liquid-helium temperature. Low-current devices give slightly better signal-to-noise ratios and therefore those units are used in the preamplifier. The selection process is, therefore, obviously simple.

More details on the germanium JFET's and the rest of the preamplifier circuit can be found in Refs. 3 and 4.

The coupling between the detector and the input stage is ac, so as to provide more flexibility in the operating conditions (temperature and bias) of the detector; dc coupling should be advantageous in cases when the optimum temperature of the detector is very low. The resistors R_1 and R_2 are kept close to 4.2°K, and their resistance at that temperature is 400 MΩ and 650 MΩ, respectively. The capacitor C_1 is a mica capacitor and its variation with temperature is negligible. The temperatures of the detector and FET's are very close and, therefore, thermoelectric effects in the coupling network are minimized.

The resolution of the preamplifier was checked with the conventional pulse generator test, using a 0.5 pF testing capacitor. The result obtained was 0.28-0.3 keV FWHM (Ge) with a slope of 0.018 keV/pF. The low sensitivity to external capacitance is a result of a relatively high input capacitance of the FET's (10-15 pF).

THE CRYOSTAT

A cross-sectional drawing of the lower part of the cryostat is shown in Fig. 4. The inner chamber contains liquid helium and is made of stainless steel. A liquid-nitrogen-cooled thermal-radiation shield, made of copper, completely surrounds the liquid-helium chamber. The liquid-nitrogen (LN) chamber is not shown. The vacuum chamber is made of aluminum.

In the lower part of the cryostat there are four identical ports placed every 90 deg. Each of the port cover plates is used for a different purpose as follows: 1) beryllium window for radiation entrance, 2) high-voltage connector, 3) preamplifier connector, and 4) connector for the heater resistors.

A liquid-helium thermal-radiation shield is placed around the detector. A Mylar strap (not shown) holds the detector onto the detector plate and supplies pressure for the electrical contact shown touching the right side of the detector. The high voltage is applied to the detector via the detector-plate holder. The detector-plate holder is insulated from the L-shaped bracket by the sapphire rod. Figure 5 is a photograph of the L-shaped bracket and the detector assembly. We use many of the parts previously described by C. E. Miner.[11]

The temperature of the detector is controlled by the two heater resistors placed between the liquid-helium chamber and the L-shaped bracket. The heater resistors connected in series, are 50 Ω 1% metal-film elements, which maintain their resistance at 4.2°K within a few percent of room temperature value. By placing a temperature-calibrated resistor on a dummy detector, the current flowing in the heater is calibrated to the temperature at the detector. By monitoring the heater current we were able to make our measurements at different temperatures without introducing undue noise caused by the additional wires to a thermometer resistor. The accuracy of the measured temperature is ±1°K. The lowest temperature attainable under these conditions is 12°K.

The germanium FET's are placed directly in the liquid helium and their connections are made via a feedthrough plate (Fig. 6). This plate is a Varian rotatable conflat flange (No. 954-5072). The feedthroughs have good vacuum seals and are chosen for low capacitance and relative immunity to thermal shock. The feedthrough for the input gate lead has a glass insulator and capacitance of 1 pF. The others have alumina insulators and have approximately 3 pF capacitance. The components of the gate circuit and the detector are placed in the vacuum chamber as indicated. This arrangement provides the lowest noise operation of the FET's and prevents the thermal radiation of the FET's from reaching the detector. We choose FET's with relatively low I_{DSS} (5 mA at room temperature) for noise considerations, low heat dissipation, and minimal loss of liquid helium.

The liquid-helium reservoir contains approximately 1.5 liters of liquid helium. This amount of the coolant lasts 8 hr with the FET's operating and 16 hr with the FET's off. Because the liquid helium cools the liquid nitrogen, there is very little LN boiling and consequently less microphonics. The liquid-helium-cooled surfaces are good cryopumps and no external pumping is required to maintain good vacuum. This means that we have no extraneous microphonics caused by mechanical vibrations of external pumps nor electrical noise caused by the high voltage of ion pumps.

PERFORMANCE OF THE SPECTROMETER

The spectrometer was tested with three different germanium detectors. Two of the detectors were low-capacitance (~2.5 pF), thin-window devices made at the Lawrence Radiation Laboratory, Berkeley.[12] The two were produced from different ingots and had different histories. The third detector was RCA's encapsulated unit-type SJGG 7/30 having capacitance of approximately 12 pF. All three detectors were tested for the temperature dependence of their resolution, and the results obtained are given in Fig. 7. The pulse-shaping time constants of the main amplifier were 5 μsec integration and differentiation. The source used was ^{57}Co and the detectors were operated at their optimum bias voltages. When cooled with liquid nitrogen (detector temperature between 80 and 90°K) the proper operating voltage of the detectors was lower and in the case of detector No. 1, the change was dramatic. The Berkeley detectors operated with bias around 600 V and the RCA detector with 540 V.

The best results were obtained with detector No. 1 -- 0.68 keV at 12°K and with bias voltage of 1200 V. With 1500 V the resolution deteriorated only slightly and, thus, lower temperature of operation could be advantageous. Detector No. 2 showed somewhat excessive noise at 57°K; its optimum temperature was 22°K. The RCA detector had optimum temperature of 32°K and its best resolution for ^{57}Co was 0.93 keV.

The spectrometer using detector No. 1 was tested with other low-energy sources as ^{55}Mn x rays, ^{241}Am (Np x rays) and ^{68}Er x rays. The K_α and K_β lines of ^{55}Mn (Fig. 8), only 0.6 keV apart are measured with 0.405 keV FWHM. The resolution for the L_α line ($L_{\alpha 1}$ = 13.96 keV, $L_{\alpha 2}$ = 13.78 keV) of the more complicated spectrum of ^{241}Am (see Ref. 4) was 0.44 keV. Figure 9 shows the x rays of ^{68}Er. We see that the K_α doublet, 0.9 keV apart, is well resolved and the $K_{\beta 1}$ line (55.78 keV) is measured with 0.495 keV resolution.

The operation of the germanium detector with high bias voltages causes an increase in microphonics. In the described spectrometer, two distinct frequencies of 200 Hz and 1 kHz were observed.

TRAPPING EFFECTS

Semiconductor detectors, especially those from compound materials,[13] suffer from trapping effects. In germanium these effects are particularly significant at the hypercryogenic temperatures, due to the increased capture cross sections of the trapping centers (σ_t). In the germanium lattice, any foreign atoms or irregularities, such as dislocations, having energy levels in the band-gap may act as trapping centers. For a single trapping level, the probability of detrapping is proportional to exp $(-\Delta E/kT)$, where ΔE is the activation energy of the trap and T the temperature of the lattice. The decreasing probability of detrapping at hypercryogenic temperatures causes the appearance of a slow-rising component in the output pulse of the detector. The waveform of typical output pulses showing the effect of trapping is given in Fig. 10. The amplitude of the fast component V_f decreases with temperature, due to the increase of the capture cross section of the trapping centers. The average value of the time constant (τ_s) of the slow component increases with decreasing temperature, due to the decreasing probability of detrapping.

Output pulses exhibiting slow rising components were observed[5] in germanium detectors below 20°K and in GaAs and CdTe detectors at room temperature.[13] We observed these pulses with the described spectrometer in the range of detector temperatures of 80 to 12°K. The number of such pulses increases noticeably as the temperature is reduced. At hypercryogenic temperatures the average time constant of the slow component is very large (~50 μsec), causing a reduced amplitude to most of the affected pulses. This in turn produces distinct satellite peaks in the observed spectrum, as can be seen in Fig. 11. In that figure several spectra of ^{241}Am are shown, concentrating on the 59.57-keV trapped γ rays. The spectra were taken at different temperatures of the detector with constant detector bias of 1500 V and integration and differentiation time constants of 5 μsec. We believe that the appearance of three distinct satellite peaks for a single-energy γ ray is due to different trapping centers. From Fig. 11 it can be seen that the apparent energy (pulse height) of the satellite peaks increases with temperature. This is a combined result of decreased σ_t and τ_s. By computing the total amount of counts and the counts under the satellite peaks, the relative variation of σ_t (assuming the same σ_t for the different traps) with temperature was calculated and is given in Fig. 12.

As expected, use of shorter differentiation and integration time constants in the amplifier (1 μsec) gives satellite peaks of lower energy (Fig. 13). By measuring the variation of τ_s with temperature, the activation energies, ΔE, of the traps can be deduced.

The energy of the satellite peaks varies also with the bias of the detector, as can be seen in Fig. 14. This figure shows the ^{241}Am spectra with the detector at 22°K for electric fields of 2 and 2.5 kV/cm. The variation in trapping rates at this temperature and such high fields may indicate hole trapping. Electron drift velocity is already saturated at the stated conditions.[5]

Using a collimated source (approximately 1 mm in diameter), we were able to ascertain that the trapping centers are concentrated in one edge of the detector. Numerous etchings of the detector did not eliminate the satellite peaks,[14] indicating bulk trapping centers.

In conclusion, we can say that operation of the germanium detector at hypercryogenic temperatures may offer valuable information on the trapping centers and their characteristics in this material. The presented study of trapping effects is by no means complete and we hope it will be continued. Similar study can be performed on silicon detectors, so as to provide better understanding of the trapping effects in that material. The collected information may prove important not only in the field of radiation detectors, but also in the much broader area of semiconductor devices.

CONCLUSIONS

The temperature dependence of the parameters of lithium-compensated germanium detectors was analyzed for temperatures below 77°K. A decrease in noise and capacitance is accompanied by an increase in trapping as the temperature is lowered. An optimum temperature exists in the range between 10 and 35°K for individual detectors.

A high-resolution spectrometer was built with a germanium detector at its optimum temperature and a liquid-helium-cooled germanium JFET preamplifier. Resolutions of the order of 0.4 keV were obtained for low-energy x rays and 0.68 keV for the γ rays of ^{57}Co.

The hypercryogenic spectrometer was used to study some aspects of the trapping effects in germanium. We believe that such study will provide important information for further improvement of semiconductor detectors.

ACKNOWLEDGMENTS

The authors would like to thank Dr. R. H. Pehl for valuable discussions. The technical assistance of J. A. Mendes, W. L. Crowder, and R. C. Jared is greatly appreciated. We wish to acknowledge the valuable help of R. E. Hintz, C. E. Miner, D. F. Malone, G. G. Young, and F. Valledon with the cryostat. This work was done under auspices of the U. S. Atomic Energy Commission.

REFERENCES

1. E. Elad, Nucl. Instr. Methods 37, 327 (1965).
2. K. F. Smith and J. E. Cline, IEEE NS-13, No. 3, 468 (1966).
3. E. Elad and M. Nakamura, IEEE NS-14, No. 1, 523 (1967).
4. E. Elad and M. Nakamura, University of California Lawrence Radiation Laboratory Report UCRL-17818 (September 1967), presented at the 14th Nuclear Science Symposium of the IEEE, Los Angeles, October 31-November 2, 1967.
5. E. Sakai, H. L. Malm, and I. L. Fowler, AECL-2762, presented at the Gatlinburg Conference on Semiconductor Nuclear Particle Detectors and Circuits, May 15-18, 1967.
6. F. S. Goulding, Nucl. Instr. Methods 43, 1 (1966).
7. J. W. Mayer, Nucl. Instr. Methods 43, 55 (1966).
8. R. Y. Deshpande, Nucl. Instr. Methods 57, 125 (1967).
9. C. T. Sah, R. N. Noyce, and W. Shockley, Proc. IRE 45, 1228 (1957).
10. A. S. Grove, Physics and Technology of Semiconductor Devices (John Wiley & Sons, Inc., New York, 1967), p. 301.
11. C. E. Miner, Nucl. Instr. Methods 55, 125 (1967).
12. R. H. Pehl, D. A. Landis, and F. S. Goulding, IEEE NS-13, No. 3, 274 (1966).
13. W. Akutagawa, K. Zanio, and J. W. Mayer, Nucl. Instr. Methods 55, 383 (1967).
14. J. P. Hurley, J. M. Mathiesen, and V. L. Dagragnano, Nucl. Instr. Methods 57, 109 (1967).

FIGURE CAPTIONS

Fig. 1. Equivalent circuit of lithium-compensated germanium detector.

Fig. 2. The input stage of the preamplifier.

Fig. 3. Transconductance of TIXM12 versus temperature.

Fig. 4. A cross section of the cryostat.

Fig. 5. The holder of the detector.

Fig. 6. Low-capacitance feedthrough plate.

Fig. 7. Resolution of germanium detectors in the hypercryogenic region.

Fig. 8. x-Ray spectrum of ^{55}Mn. (Energy in keV.)

Fig. 9. x-Ray spectrum of ^{68}Er. (Energy in keV.)

Fig. 10. The waveform of the output pulse of the preamplifier with and without trapping.

Fig. 11. Satellite peaks versus temperature of the detector.

Fig. 12. Trapping cross section in the hypercryogenic region.

Fig. 13. Satellite peaks for different pulse-shaping time constants.

Fig. 14. Satellite peaks versus electric field in the detector.

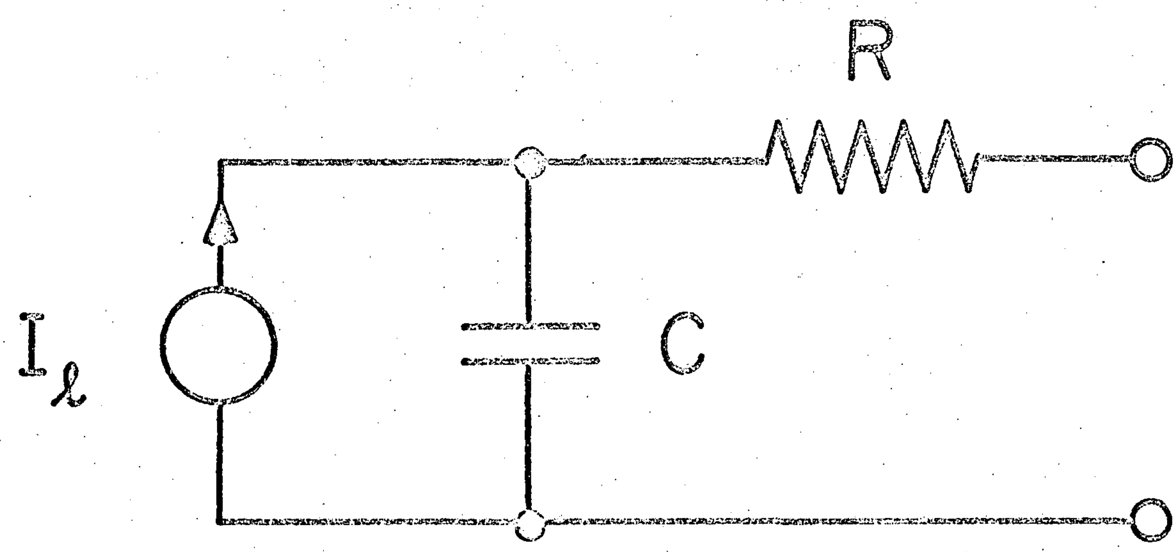

XBL682-1715

Fig. 1

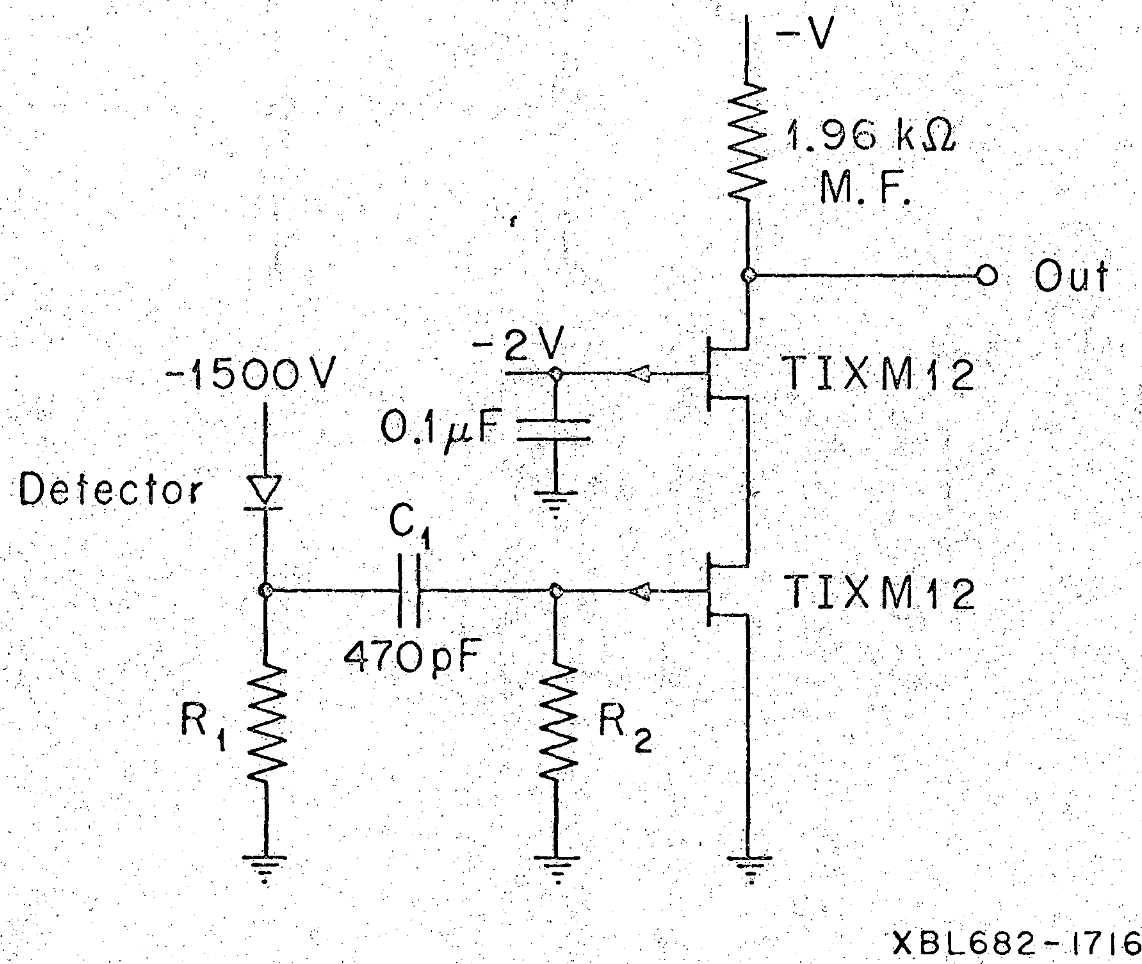
-V
1.96 kΩ
M. F.
Out
-2V
TIXM12
-1500V
0.1 μF
Detector
C_1
TIXM12
470 pF
R_1
R_2
XBL682-1716

Fig. 2

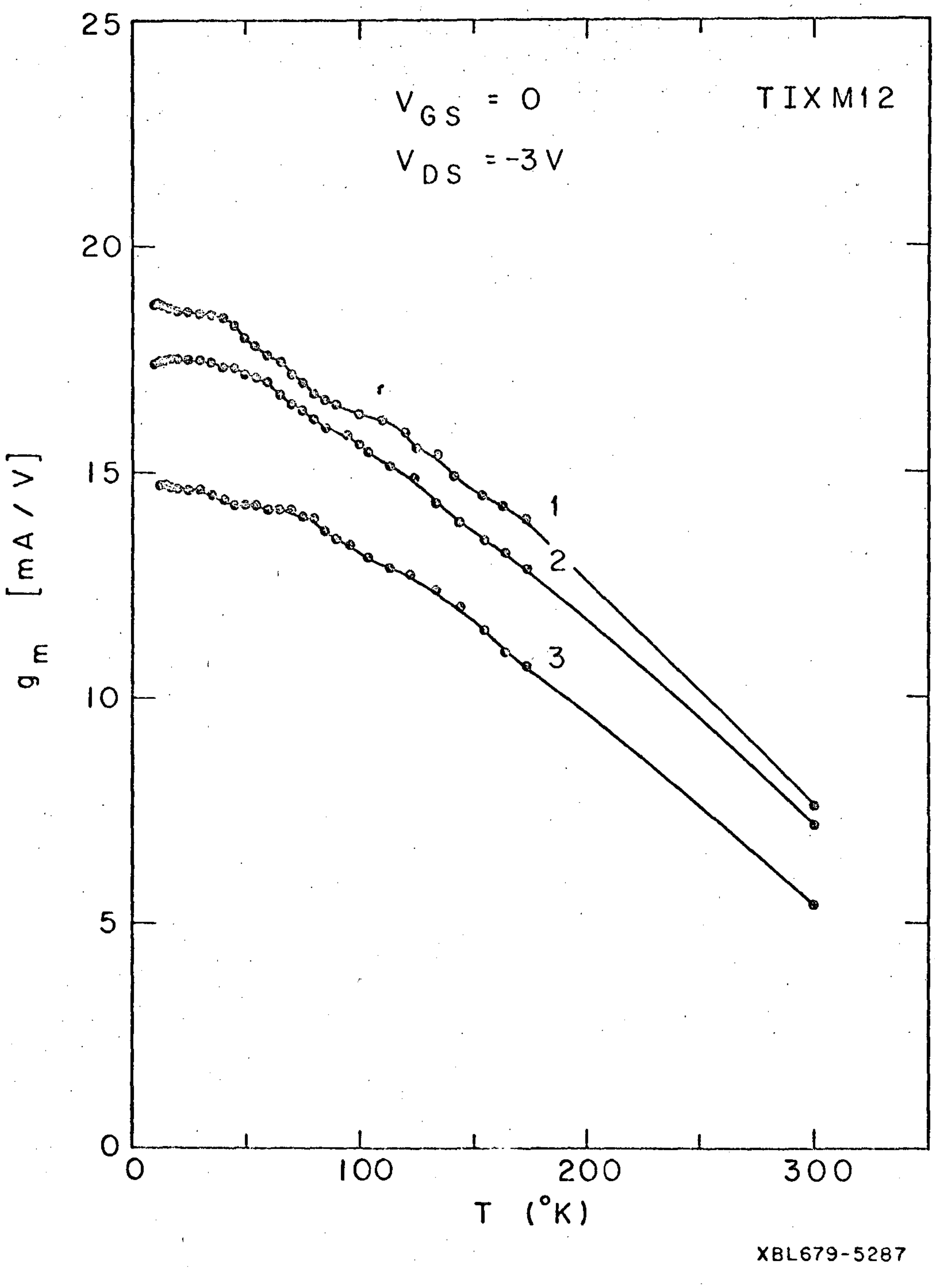
25
20
15
10
5
0
V_{GS} = 0
V_{DS} = -3 V
TIXM12
1
2
3
g_m [mA / V]
0
100
200
300
T (°K)
XBL679-5287

Fig. 3

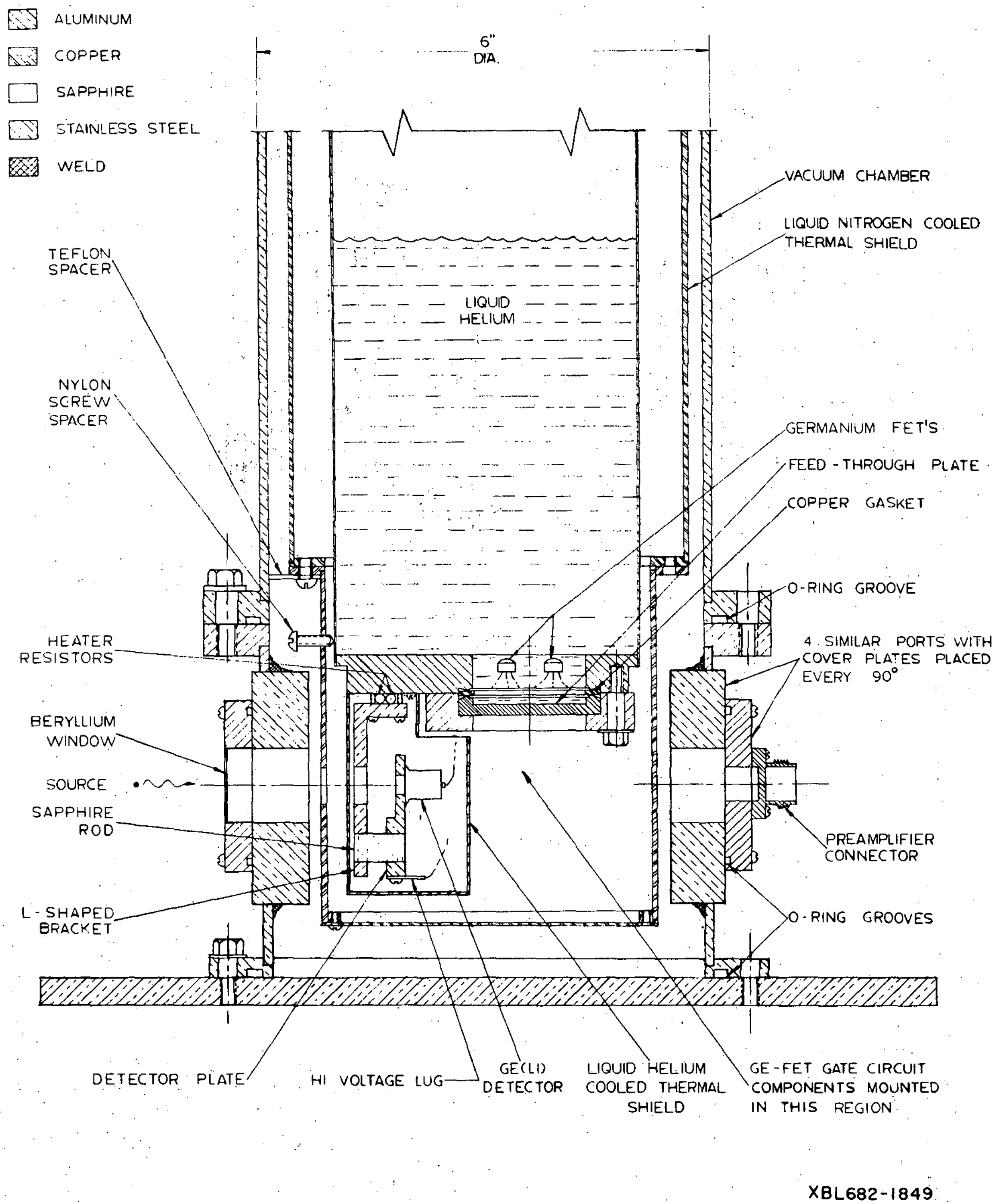
ALUMINUM
COPPER
SAPPHIRE
STAINLESS STEEL
WELD
6" DIA.
VACUUM CHAMBER
LIQUID NITROGEN COOLED THERMAL SHIELD
TEFLON SPACER
LIQUID HELIUM
NYLON SCREW SPACER
GERMANIUM FET'S
FEED-THROUGH PLATE
COPPER GASKET
O-RING GROOVE
HEATER RESISTORS
4 SIMILAR PORTS WITH COVER PLATES PLACED EVERY 90°
BERYLLIUM WINDOW
SOURCE
SAPPHIRE ROD
PREAMPLIFIER CONNECTOR
L-SHAPED BRACKET
O-RING GROOVES
DETECTOR PLATE
HI VOLTAGE LUG
GE(LI) DETECTOR
LIQUID HELIUM COOLED THERMAL SHIELD
GE-FET GATE CIRCUIT COMPONENTS MOUNTED IN THIS REGION
XBL682-1849

Fig. 4

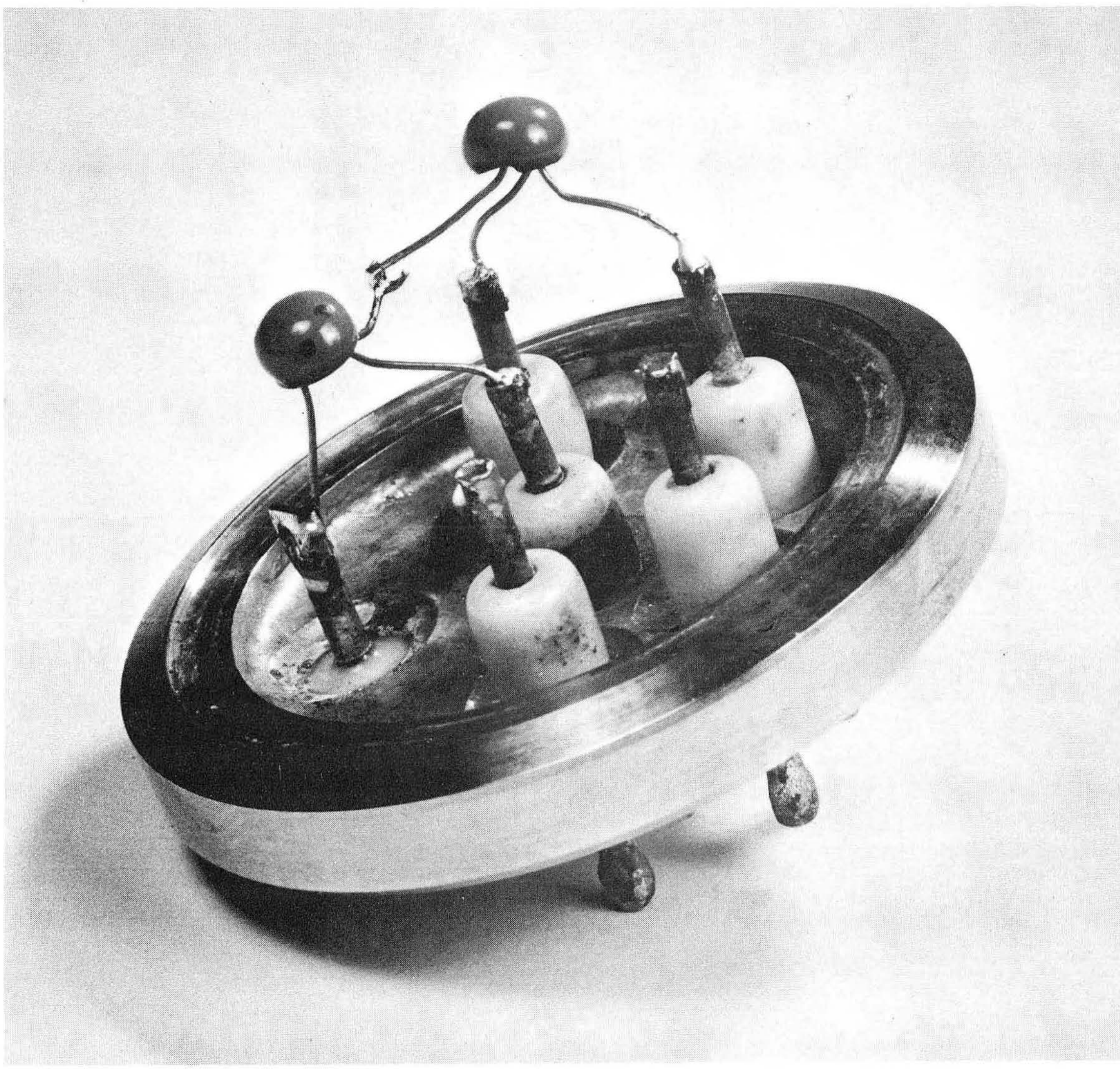

XBB 681-420

Fig. 5

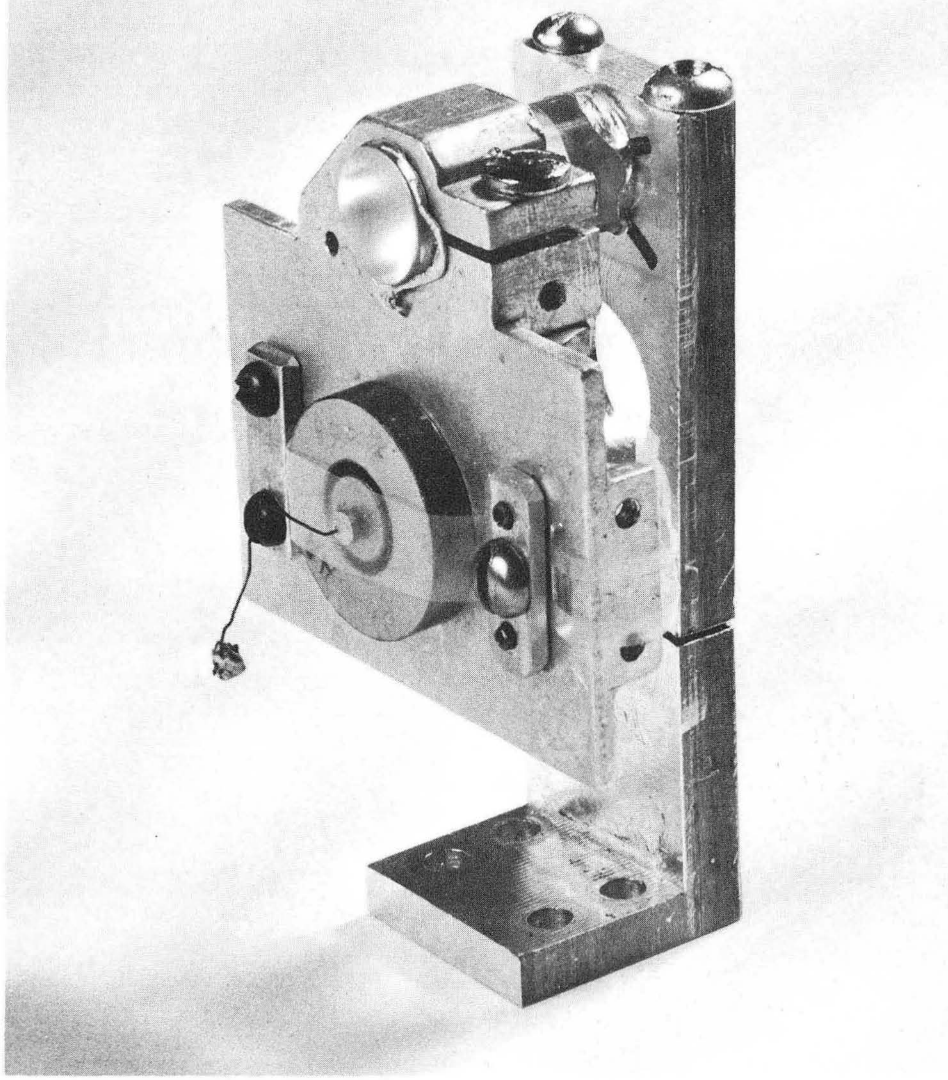

XBB 681-419

Fig. 6

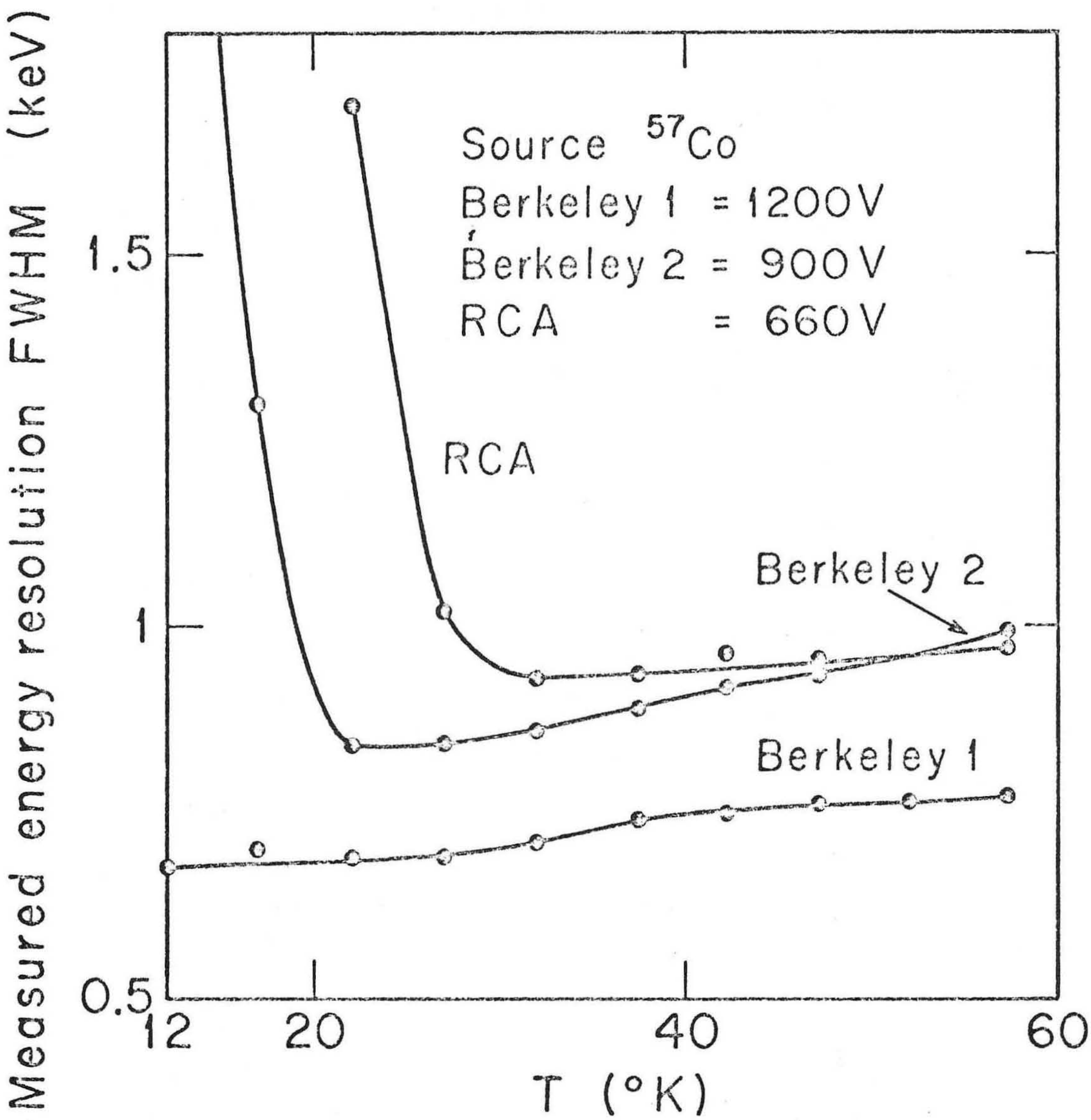
Measured energy resolution FWHM (keV)
1.5
1
0.5
12
20
40
60
T (°K)
Source ^{57}Co
Berkeley 1 = 1200V
Berkeley 2 = 900V
RCA = 660V
RCA
Berkeley 2
Berkeley 1
XBL682-1717

Fig. 7

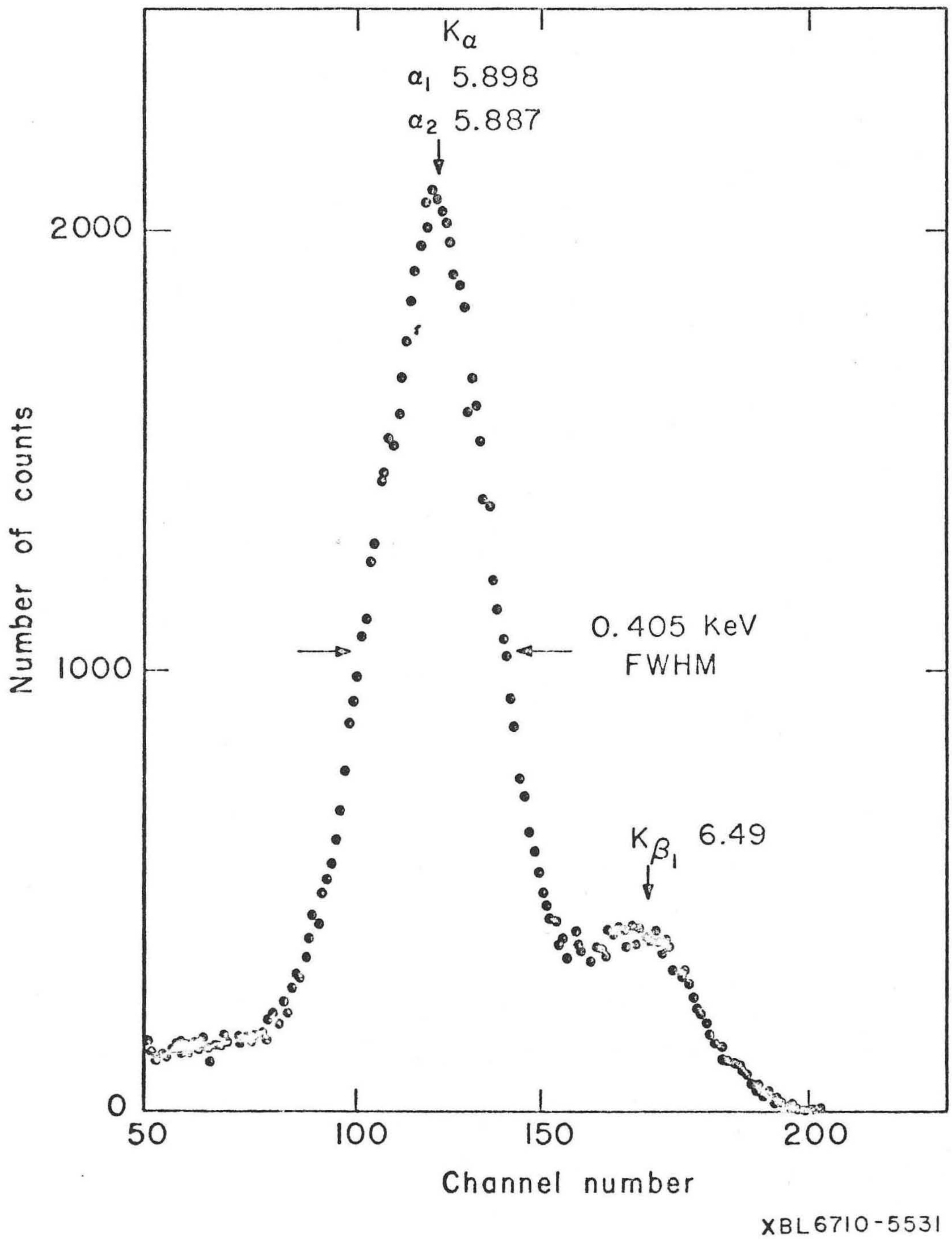
Kα
α1 5.898
α2 5.887
0.405 KeV
FWHM
Kβ1 6.49
2000
1000
0
Number of counts
50
100
150
200
Channel number
XBL6710-5531

Fig. 8

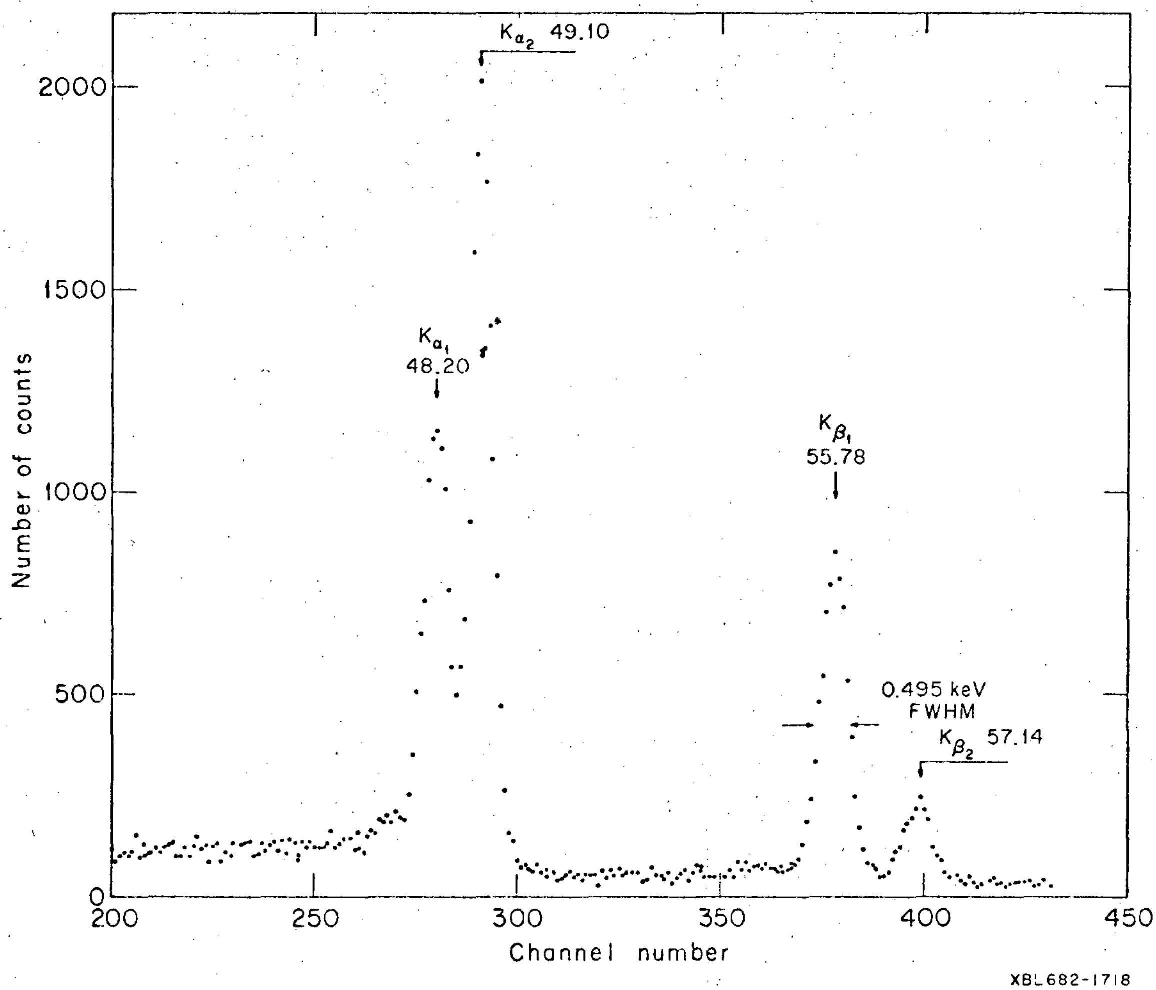

K_{α_2} 49.10
2000
1500
1000
500
0
K_{α_1} 48.20
K_{β_1} 55.78
0.495 keV FWHM
K_{β_2} 57.14
Number of counts
200
250
300
350
400
450
Channel number
XBL682-1718

Fig. 9

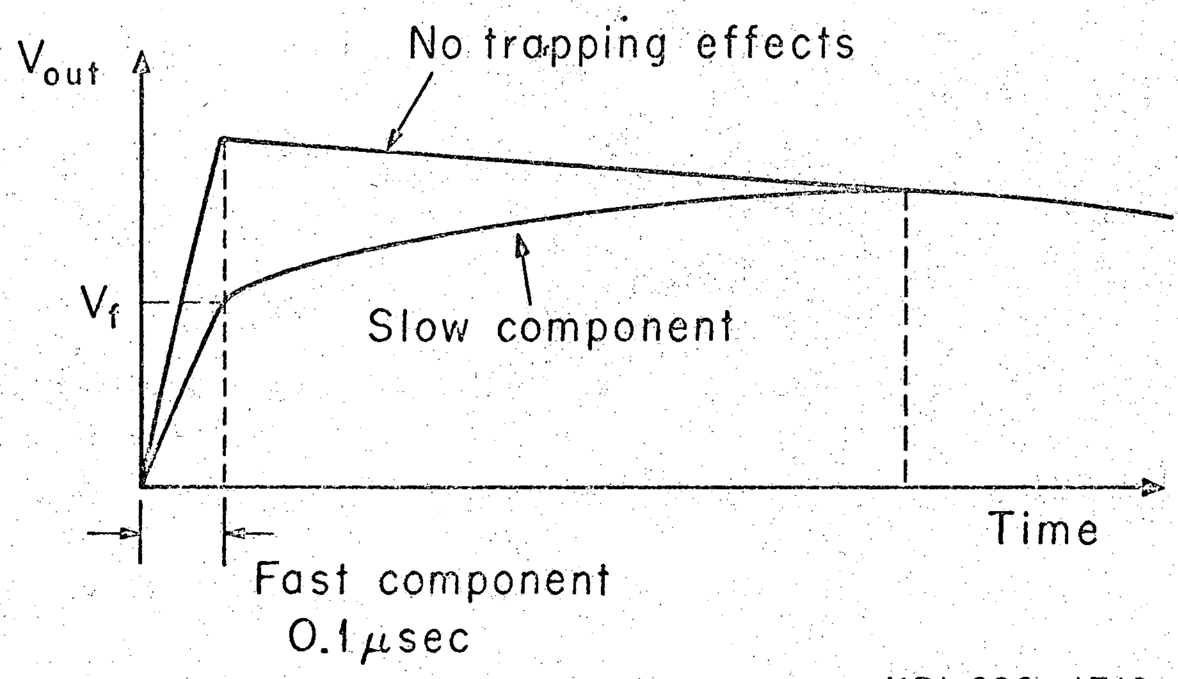
No trapping effects
V_{out}
V_f
Slow component
Time
Fast component
0.1 μsec
XBL 682-1719

Fig. 10

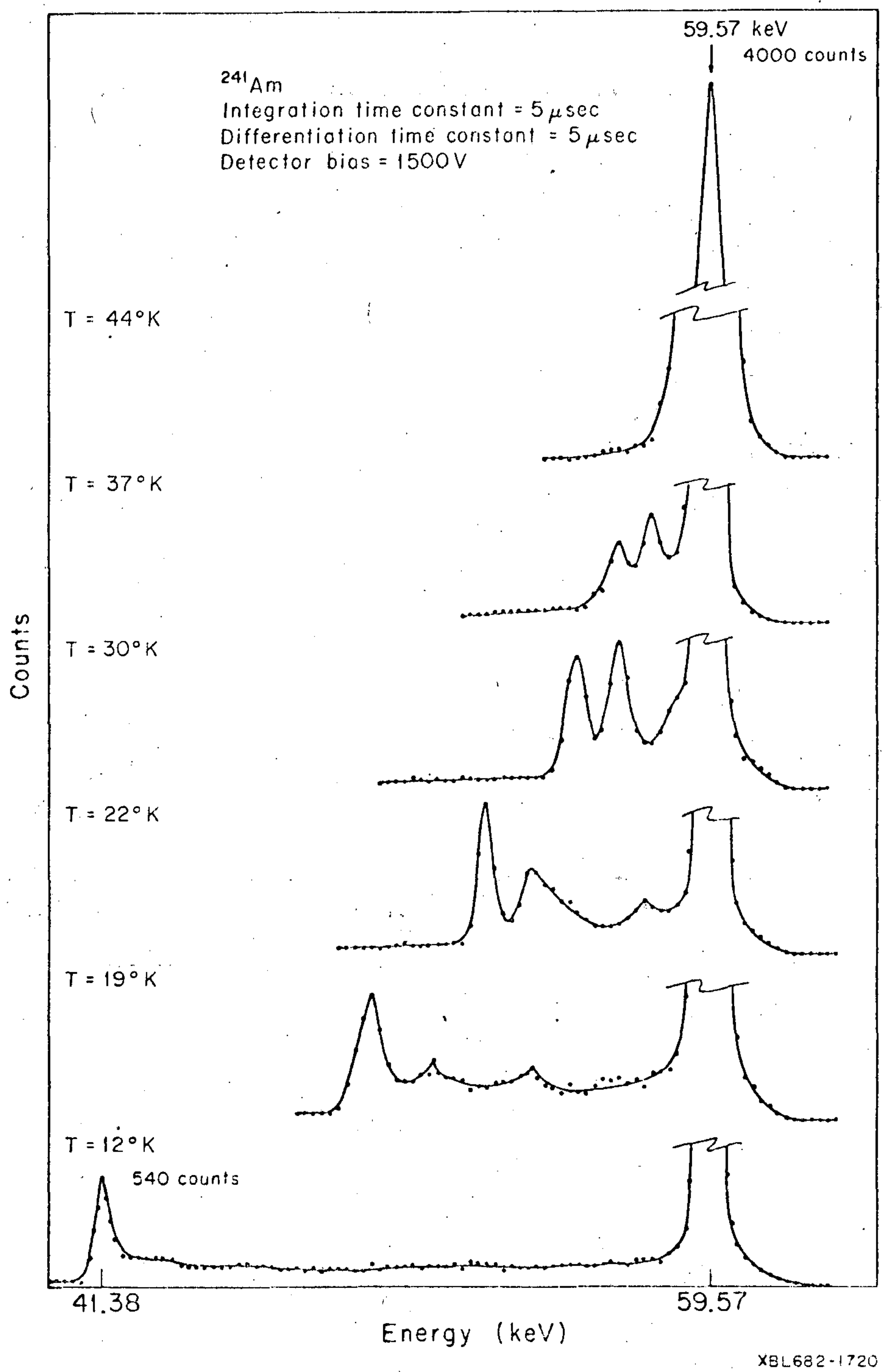
59.57 keV
4000 counts
^{241}Am
Integration time constant = 5 μsec
Differentiation time constant = 5 μsec
Detector bias = 1500V
T = 44°K
T = 37°K
T = 30°K
T = 22°K
T = 19°K
T = 12°K
540 counts
Counts
41.38
59.57
Energy (keV)
XBL682-1720

Fig. 11

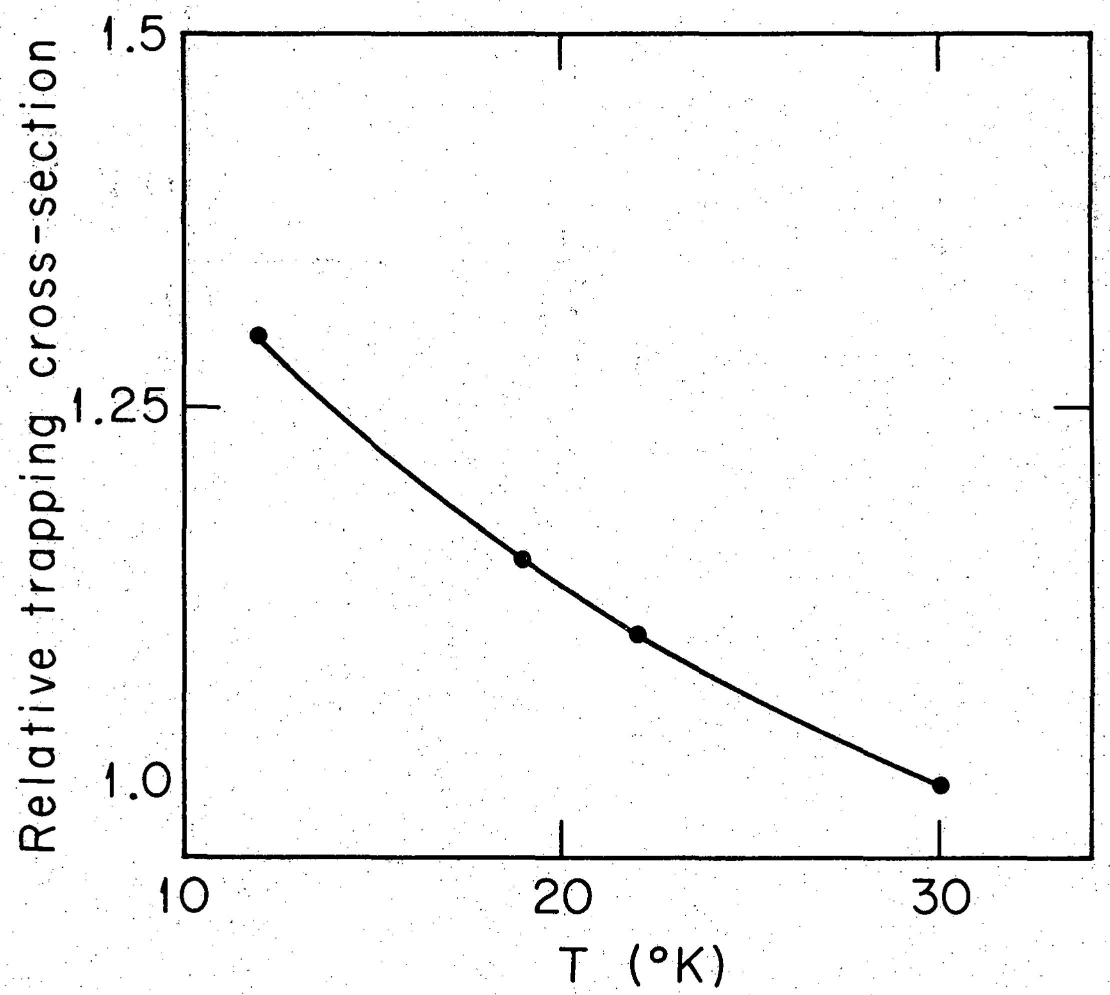
1.5
1.25
1.0
Relative trapping cross-section
10
20
30
T (°K)
XBL682-1846

Fig. 12

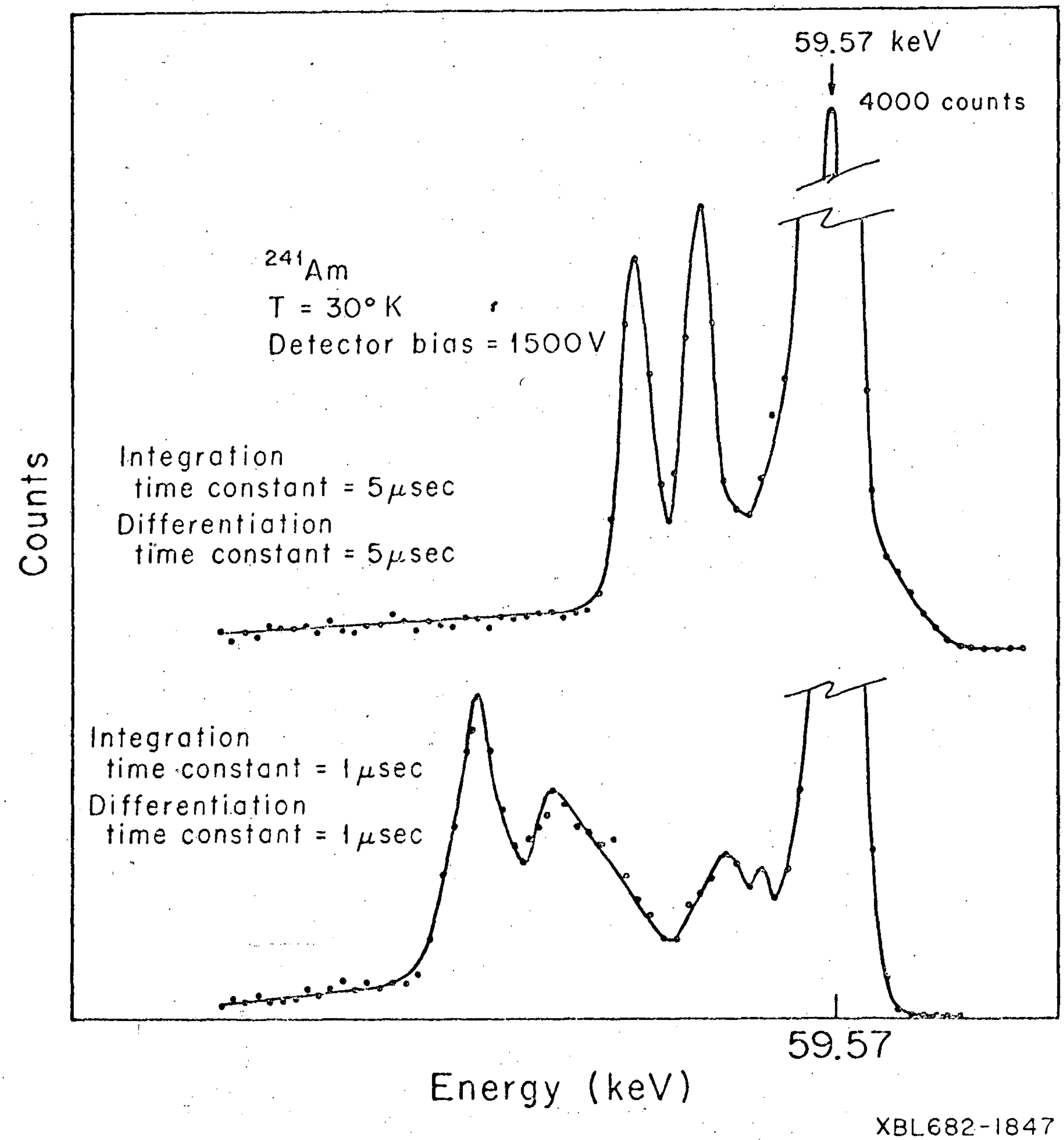
59.57 keV
4000 counts
^{241}Am
T = 30° K
Detector bias = 1500V
Integration time constant = 5 μsec
Differentiation time constant = 5 μsec
Integration time constant = 1 μsec
Differentiation time constant = 1 μsec
Counts
59.57
Energy (keV)
XBL682-1847

Fig. 13

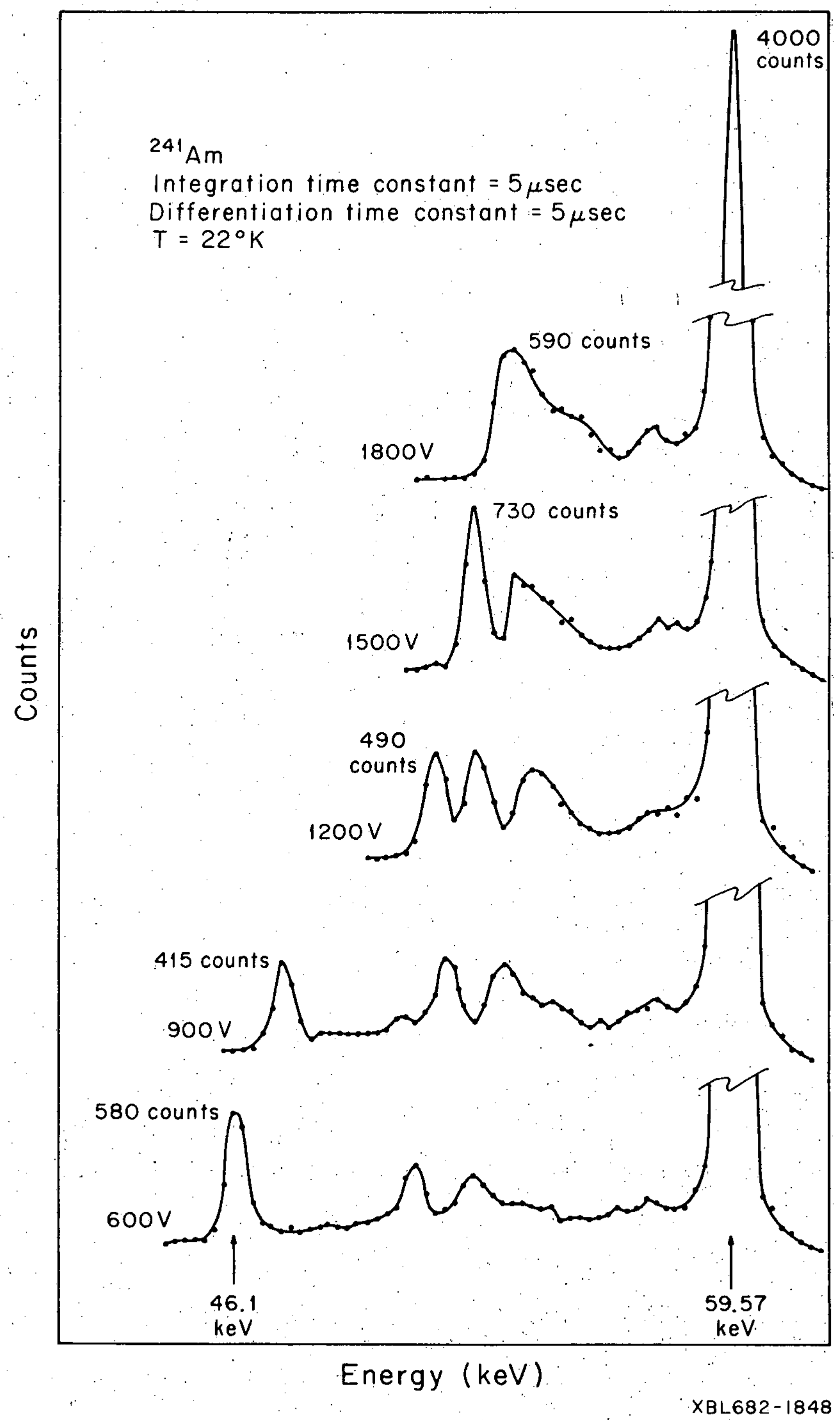
4000
counts
^{241}Am
Integration time constant = 5μsec
Differentiation time constant = 5μsec
T = 22°K
590 counts
1800V
730 counts
1500V
490
counts
1200V
415 counts
900V
580 counts
600V
46.1
keV
59.57
keV
Counts
Energy (keV)
XBL682-1848

Fig. 14